24th COBEM - 2017

24th ABCM International Congress of Mechanical Engineering
December 3-8, 2017, Curitiba, PR, Brazil

COBEM-2017-2239

A STRIP-YIELD ALGORITHM TO PREDICT FATIGUE CRACK CLOSURE AND GROWTH

Samuel Elias Ferreira
Pontifícia Universidade Católica do Rio de Janeiro, PUC-Rio, Department of Mechanical Engineering, Rio de Janeiro, Brazil
ferreirase@hotmail.com

Jaime Tupiassú Pinho de Castro
Pontifícia Universidade Católica do Rio de Janeiro, PUC-Rio, Department of Mechanical Engineering, Rio de Janeiro, Brazil
jtcastro@puc-rio.br

Marco Antonio Meggiolaro
Pontifícia Universidade Católica do Rio de Janeiro, PUC-Rio, Department of Mechanical Engineering, Rio de Janeiro, Brazil
meggi@puc-rio.br

Abstract. *Strip-yield models, which assume that the effective stress intensity range (ΔK_{eff}) is the driving force for fatigue crack propagation, are widely used for fatigue design purposes. Since originally proposed by Newman in 1981, a few strip-yield algorithms have been developed and implemented in commercial or proprietary codes, to calculate fatigue crack opening stresses created by plasticity-induced crack closure. Since such codes are not properly discussed in the open literature, here an academic strip-yield algorithm especially developed to calculate ΔK_{eff} under constant and variable amplitude loading is described in detail. Like in similar commercial codes, this homemade algorithm uses equations for plastic zones, element displacements, and opening stresses proposed by Newman, and combine them with a proper calculation procedure. Moreover, its capability to reproduce measured opening loads and fatigue crack growth rates is also analyzed.*

Keywords: *strip-yield model, crack-opening stress, variable amplitude load*

1. INTRODUCTION

After identifying plasticity-induced fatigue crack closure under tensile loads, Elber (1971) speculated that the effective stress intensity range $\Delta K_{eff} = K_{max} - K_{op}$ (instead of $\Delta K = K_{max} - K_{min}$) would be the actual fatigue crack driving force, where K_{max} and K_{min} are the maximum and the minimum values of the applied stress intensity factor (SIF), and $K_{op} \geq K_{min}$ is the SIF value that completely opens the fatigue crack. Despite its many limitations (Vasudevan et al. 2003, Meggiolaro and Castro, 2003) this idea still is supported by many fatigue experts, because it can rationalize many load order effects induced by variable amplitude loadings (VAL), like delays and arrests of fatigue crack growth (FCG) after overloads, as well as FCG accelerations after underloads (Skorupa, 1999).

Indeed, based in a good correlation between ΔK_{eff} and FCG rates (da/dN) reported by von Euw et al. in 1972, shortly after Elber proposed it, this idea was promptly accepted in the fatigue community. Since then, many experimental works have been performed to test ΔK_{eff} predictions under several conditions, see e.g. Skorupa (1998) for a quite comprehensive although somewhat biased review of the work done in the last century.

The most successful models that use ΔK_{eff} principles for fatigue design purposes are the so-called strip-yield models (SYM) based on the Dugdale (1960) idea. Dill and Saff (1976), Newman Jr. (1981), de Koning and Liefting (1988), and Wang and Blom (1991) are examples of such SYMs. In fact, a SYM-based algorithm is included into the NASGRO software developed by the NASA team, an early example of a code used for design purposes (which used to be free, but is not anymore). Similar codes are particularly popular in the aerospace industry. The objective of this work is to describe an algorithm for SYM-based calculation procedures (Newman 1981, 1992) in a suitable code capable of estimating fatigue lives under VAL. In particular, the entire calculation procedure is presented, to clearly show how to deal with the crack closure transient behavior under VAL, an issue not properly discussed in the open literature, due to its commercial applications. K_{op} values calculated by the proposed algorithm are compared with Newman's estimates for constant amplitude loads (CAL) and with the results published by de Koning and Liefting (1988) for VAL.

2. SYM ALGORITHM DESCRIPTION

SYMs numerically estimate the crack opening SIFs K_{op} needed to find ΔK_{eff} using the classic Dugdale model (1960), modified to leave plastically deformed material around the faces of the advancing fatigue crack. Newman´s original SYM (1981) is based on Elber's plasticity-induced crack closure idea. It was developed for a finite plate with a central crack (an M(T) specimen) remotely loaded by a uniform tensile stress σ_n. The plastic zone size pz and the surface displacements are obtained by the superposition of two linear elastic problems: (i) a cracked plate loaded by a remote uniform nominal tensile stress σ_n (Fig. 1a), and (ii) by a uniform distributed stress σ applied over crack surface segments (Fig. 1b).

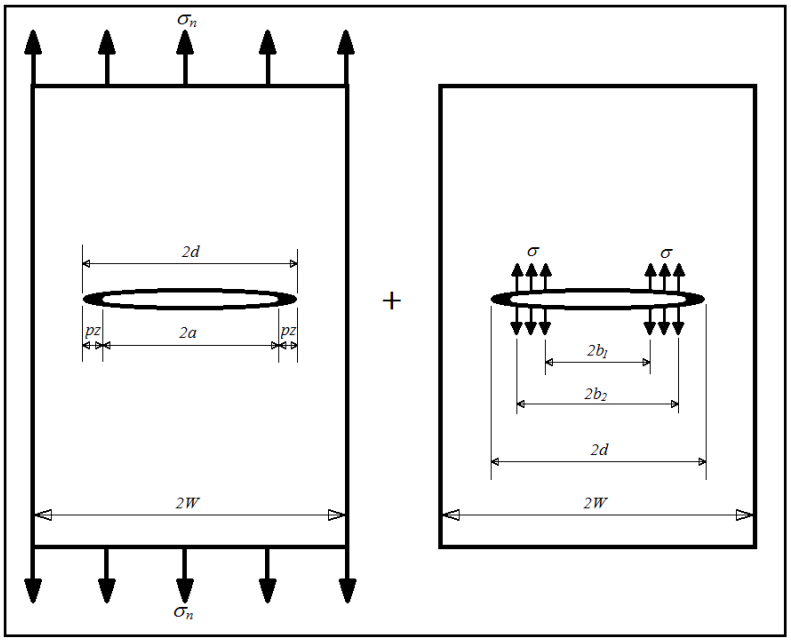

Figure 1. (a) M(T) with a crack of size $2(a + pz)$ loaded by a remote tensile stress σ_n; and (b) M(T) with a crack of size $2(a + pz)$ loaded by symmetrical distributed stresses σ over two segments near the crack tips (Newman, 1981).

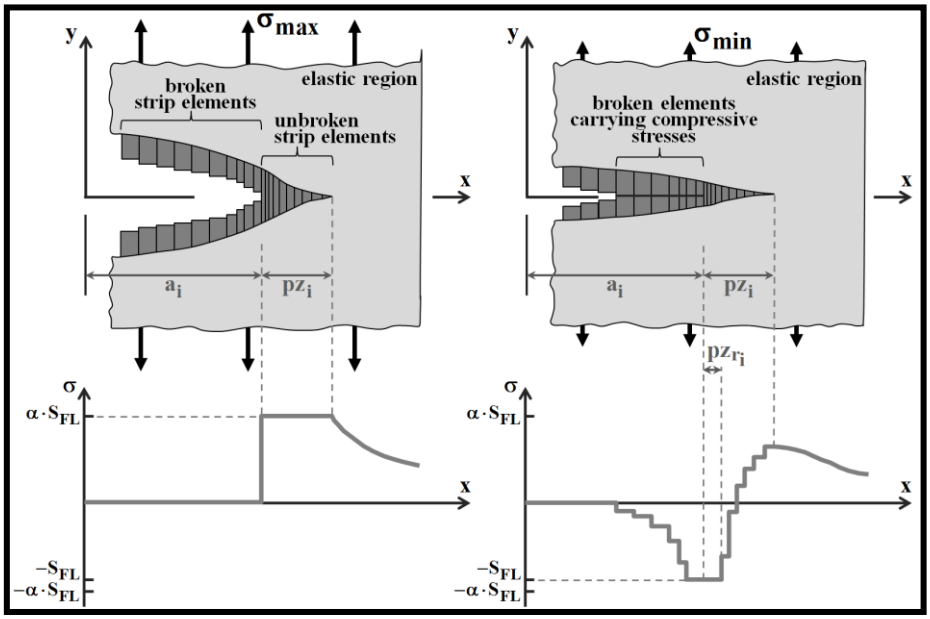

Figure 2: Crack surface displacements and stress distribution along the crack line (Newman Jr, 1981).

Figure 2 shows the crack surface displacements and the stress distributions around the crack tip at the maximum σ_{max} and minimum σ_{min} applied stresses. It is composed of three regions: (1) a linear elastic region containing a fictitious crack of half-length $a + pz$; (2) a plastic region of length pz; and (3) a residual plastic deformation region along the crack surface.

The plastic zone pz is discretized in a series of rigid-perfectly plastic 1D bar elements, which are assumed to yield at the flow strength of the material, $S_F = (S_Y + S_U)/2$, to somehow account for the otherwise neglected strain-hardening

effects. These elements are either intact inside the plastic zone or broken at the crack wake, but storing their residual plastic deformations. If they are in contact, the broken bar elements can carry compressive stresses, therefore they can yield in compression when their stresses reach $-S_F$. The (broken) elements along the crack face that are not in contact do not affect the crack surface displacements, or carry stresses.

The SYM uses a constraint factor α to increase the tensile flow stress S_F in the unbroken elements along the plastic zone during loading in thick plates. This is done to somehow consider the effects of the actually 3D stresses around the crack tip, caused by plastic restrictions when the plate is thick and cannot be assumed to work under plane stress *pl-σ*. So, this constraint factor should vary from $\alpha = 1$ for plane-stress to up to $\alpha = 1/(1 - 2\nu) \cong 3$ for plane-strain limit conditions, where ν is Poisson's coefficient (albeit α is often used as a data-fitting parameter in practical applications). Since there is no crack-tip singularity when the crack closes, this constraint factor is not used to modify the compressive yield stress during unloading, assuming the conditions around the crack tip tend to remain uniaxial.

The coordinate system shown in Fig. 2 is fixed and its origin lies at the center of the central crack, whose length is $2a$. Due to symmetry, only one quarter of the plate needs to be analyzed. Equation (1) governs the system response by requiring compatibility between the LE part of the cracked plate and all bar elements. When the length L_j of the broken wake elements along the crack faces is larger than their displacement V_j under σ_{min}, they come into contact and induce a stress σ_j needed to force $V_j = L_j$. The influence functions $f(x_i)$ and $g(x_i, x_j)$ used in Eq. (1) are related to the plate geometry and its width correction, as expressed in Eqs. (2-4).

$$V_i = \sigma_n f(x_i) - \sum_{j=1}^{n} \sigma_j \cdot g(x_i, x_j) \tag{1}$$

$$f(x_i) = [2(1-\eta^2)/E]\sqrt{(d^2 - {x_i}^2)\sec(\pi d/2W)} \tag{2}$$

$$g(x_i, x_j) = G(x_i, x_j) + G(-x_i, x_j) \tag{3}$$

$$G(x_i, x_j) = \frac{2(1-\eta^2)}{E}\left\{(b_2 - x_i)\cdot cosh^{-1}\left(\frac{d^2 - b_2 x_i}{d|b_2 - x_i|}\right) - (b_1 - x_i)\cdot cosh^{-1}\left(\frac{d^2 - b_1 x_i}{d|b_1 - x_i|}\right) + \sqrt{d^2 - x_i^2}\cdot \right.$$
$$\left. [sin^{-1}(b_2/d) - sin^{-1}(b_1/d)]\cdot\left[\frac{sin^{-1}B_2 - sin^{-1}B_1}{sin^{-1}(b_2/d) - sin^{-1}(b_1/d)}\right]\cdot\sqrt{sec\left(\frac{\pi d}{2W}\right)}\right\} \tag{4}$$

Notice that $\eta = 0$ for plane stress and $\eta = \nu$ for plane strain, and that B_1 and B_2 are calculated from Eq. (5), b_1 and b_2 from Eqs. (6) and (7), and the plastic zone pz from Eqs. (8) and (9).

$$B_k = \sin(\pi b_k/2W)/\sin(\pi d/2W) \tag{5}$$

$$b_1 = x_j - w_j \tag{6}$$

$$b_2 = x_j + w_j \tag{7}$$

$$pz = a\{(2W/\pi a)\cdot \sin^{-1}\{\sin(\pi a/2W)\cdot \sec[(\pi\sigma_n f)/(2\alpha S_F)]\} - 1\} \tag{8}$$

$$f = 1 + 0.22(a/W)^2 \tag{9}$$

In Fig. 2, the plastic zone ahead of the crack tip pz is divided into 20 bar elements with variable width ratio, namely $2w_i/pz =$ 0.01, 0.01, 0.01, 0.01, 0.015, 0.02, 0.025, 0.03, 0.035, 0.04, 0.045, 0.05, 0.058, 0.066, 0.074, 0.082, 0.09, 0.098, 0.107, 0.125, 0.15. The smallest element $n = 1$ is the closest to the crack tip, at $x = a$. After calculating the pz size induced by the peak stress σ_{max} of the current cycle, the lengths of the bar elements inside the plastic zone become:

$$L_i = V_i = \sigma_{max}\cdot f(x_i) - \sum_{j=1}^{20} \alpha \cdot S_F \cdot g(x_i, x_j) \tag{10}$$

When the plate is unloaded down to σ_{min} (Fig. 2b), the bar elements inside pz unload until some of them near the crack tip start to yield in compression, when they try to reach a stress $\sigma_j \leq -S_F$. The broken elements located inside the plastic wake formed along the crack surfaces, which store residual deformations, may come into contact and carry compressive stresses as well. Some of these elements may also yield in compression, if they try to reach $\sigma_j \leq -S_F$. The compatibility equation for the minimum applied load (σ_{min}) is expressed in Eq. 11. It can be rewritten to calculate the element stresses (Eq. 12), in which the stresses σ_i acting at each one of the n elements is calculated considering the stretched length L_i induced by the displacements caused by the previous maximum load.

$$\sum_{j=1}^{n} \sigma_j g(x_i, x_j) = \sigma_{min} f(x_i) - L_i \tag{11}$$

$$(\sigma_i)_I = \left[Sf_i - L_i - \sum_{j=1}^{i-1}(\sigma_j)_I g_{ij} - \sum_{j=i+1}^{n}(\sigma_j)_{I-1} g_{ij}\right]/g_{ii} \quad (12)$$

This system of equations is solved by Gauss-Seidel's iterative method with added constraints. The constraints are related to the idealized yield behavior in tension and compression of the bar elements inside *pz*, see Eqs. (13) and (14), and to element separation and compressive yielding for the broken elements along the plastic wake that envelops the crack surfaces, see Eqs. (15) and (16). The adopted convergence criterion for the iteration process is an error lower than $0.01*S_F$.

$$For\ x_j > a, if\ \sigma_j > \alpha S_F\ set\ \sigma_j = \alpha S_F \quad (13)$$

$$For\ x_j > a, if\ \sigma_j < -S_F\ set\ \sigma_j = -S_F \quad (14)$$

$$For\ x_j \leq a, if\ \sigma_j > 0\ set\ \sigma_j = 0 \quad (15)$$

$$For\ x_j \leq a, if\ \sigma_j < -\sigma_F\ set\ \sigma_j = -S_F \quad (16)$$

From the stresses in the elements at the minimum load, their plastic residual deformations can be recalculated using Eq. (17). For the elements not in contact, it follows that $\sigma_i = 0$ and $L_i < V_i$.

$$L_i = V_i = \sigma_{min} \cdot f(x_i) - \sum_{j=1}^{n} \sigma_j \cdot g(x_i, x_j) \quad (17)$$

The stress σ_{op} that completely opens the crack surfaces is calculated from Eqs. (18) and (19) with $k = 1$ or 2 according to Newman (1992). In these equations, a_w is the sum of the initial crack length with all element widths at the crack surface, but the width for the element n is replaced by the largest crack growth increment during the generation of Δa^*, not by the entire increment over which the opening stress is held constant.

$$\sigma_{op} = \sigma_{min} - \sum_{j=21}^{n}\left(2\sigma_j/\pi\right) \cdot [\sin^{-1} B_2 - \sin^{-1} B_1] \quad (18)$$

$$B_k = sin(\pi b_k/2W)/sin(\pi a_w/2W) \quad (19)$$

The opening stress σ_{op} is kept constant during a small arbitrary crack increment Δa^*, to save computational cost. At the maximum load, Δa^* is calculated from Eq. (20), where $R_x = R = \sigma_{min}/\sigma_{max}$ if $R > 0$ and $R_x = 0$ if $R \leq 0$. In the original FASTRAN code, the crack increment is assumed to be $\Delta a^* = 0.05 \cdot pz$, and Eq. (20) is used to improve the opening stress calculations for higher stress ratios (Newman, 1992).

$$\Delta a^* = 0.2(pz/4) \cdot (1 - R_x)^2 \quad (20)$$

The number of load cycles ΔN needed to grow the crack by this Δa^* increment (limited to 500 cycles) is calculated by the NASGRO $da/dN \times \Delta K_{eff}$ FCG rule, Eq. (21) (NASGRO, 2002), in which C_n, m, p and q are data fitting parameters, K_c is the fracture toughness, and the threshold ΔK_{th} can be estimated using Eqs. (22) and (23). ΔK_1^* is given by Eq. (24), A_0 by Eq. (25), ΔK_1 is the threshold measured at high R when the crack is closure-free, C_{th} is still another empirical data-fitting constant with different values for positive or negative (superscript p or n) values of R, and a_0 is an "intrinsic crack size" (assumed fixed, $a_0 = 0.0381mm$). ΔK_1 is also called the intrinsic threshold by ΔK_{eff} supporters, or the threshold of the maximum by the Unified Approach followers, who say that ΔK and K_{max} are the true fatigue crack driving forces (Vasudevan et al, 2003).

$$da/dN = C_n\left(\Delta K_{eff}\right)^m \cdot (1 - \Delta K_{th}/\Delta K)^p/(1 - K_{max}/K_c)^q \quad (21)$$

$$\Delta K_{th} = \Delta K_1^*\left[(1-R)/\left(1 - K_{op}/K_{max}\right)\right]^{\left(1+RC_{th}^p\right)}/(1 - A_0)^{(1-R)C_{th}^p}, R \geq 0 \quad (22)$$

$$\Delta K_{th} = \Delta K_1^*\left[(1-R)/\left(1 - K_{op}/K_{max}\right)\right]^{\left(1+R\cdot C_{th}^m\right)}/(1 - A_0)^{\left(C_{th}^p - R\cdot C_{th}^m\right)}, R < 0 \quad (23)$$

$$\Delta K_1^* = \Delta K_1[a/(a + a_0)]^{1/2} \quad (24)$$

$$A_0 = (0.825 - 0.34\alpha + 0.05\alpha^2) \cdot [\cos(\pi\sigma_{max}/2S_F)]^{1/\alpha} \quad (25)$$

To keep the number of elements reasonable, say less than 40, a lumping process along the plastic wake is used to join the bar elements, combining adjacent elements *i* and *i + 1* to form a single one when

$$2(w_i + w_{i+1}) \leq a - x_{i+1} - \Delta a^* \tag{26}$$

It follows that the elements near the crack tip are not as likely to be lumped together as those that are away from the tip. In the lumping process, the width of the lumped element is the sum of the widths of the two adjacent elements, while its length is the weighted average of the two, namely

$$L = (L_i w_i + L_{i+1} w_{i+1})/(w_i + w_{i+1}) \tag{27}$$

The model is able to estimate the nonlinear behavior of FCG observed under VAL due to plasticity-induced memory or load-order effects, assuming the crack-opening SIF K_{op} is their inductor mechanism. FCG acceleration or retardation is predicted if the actual K_{op} is lower or higher than the opening loads that would be induced under equivalent (i.e., same K_{max} and K_{min}) CAL conditions. Hence, the transient behavior of the crack-opening stresses under VAL is a direct result of the influence of the plasticity induced by the previous load cycles on the subsequent stress and displacement fields near the crack tip. In other words, to consider memory effects on FCG, it is necessary to use the previous stress and displacement fields ahead and behind the crack tip to determinate the subsequent states of stress and displacement.

The routine to calculate the stresses and displacements acting in all bar elements around the crack tip under VAL is developed based on the concept of plasticity-induced memory effects proposed by Führing and Seeger (1979). The effect of a previous loading state on a subsequent loading state ceases when the elastoplastic boundary of the previous loading is reached by the current plastic zone. The loss of the plastic memory caused by any given previous loading state occurs just when the entire initially plasticized region has yielded, since the bearing capacity of all material elements within this region is reached. In other words, if the monotonic plastic zone created by the current maximum applied stress plus the current crack length is lower than the previous monotonic plastic zone plus its associated crack length, then the history of the stresses and displacements must be used. Otherwise, the current loading sets the new stress and displacement history. Hence, memory effects occur while $a + pz \leq a_{ol} + pz_{ol}$. So, the plastic zone size is the basic quantity for describing memory effects since it governs the memory criterion as well as the stresses and displacement functions – variable *d* at Eqs. (2 and (4).

Therefore, while the memory effect criterion is satisfied if ($a + zp \leq a_{ol} + zp_{ol}$), the algorithm must first recalculate the elements' width and position based on the remaining monotonic plastic zone of the overload cycle and on the current crack size. After that, an interpolation routine estimates the displacements of each element based on the residual displacements previously stored at the overload event. With a similar procedure to find the contact stress at the minimum applied stress described by Eqs. (12)-(16), the next step is to find the element stresses using as input the displacements calculated by interpolation and by the current applied maximum stress. This interactive process results in a stress array for the elements ahead of the crack tip used to calculate the displacements of these elements. So, the stresses and displacement fields ahead of the crack tip during memory effects are obtained. The sequence of calculation steps and the flow diagram of the implemented algorithm are described in Fig. 3.

3. RESULTS AND DISCUSSION

To validate the SYM algorithm described here, its predictions are compared with results from Newman (1981, 1992) and from Koning and Liefting (1988). Predictions of crack opening stresses estimated by the proposed model are compared as well with fitting equations developed by Newman (1992), which are able to estimate the crack opening stress under CAL conditions.

Figure 4 presents results for three constraint factors (from plane stress to plane strain) and stress ratios $-1 \leq R \leq 0.8$ keeping the maximum applied stress in 135MPa. The lines are the results from the developed algorithm and the dots are from Newman's equation. The maximum difference between them is lower than 4%. Notice that the crack remains opened (since $\sigma_{op} = \sigma_{min}$) for $\alpha = 3$ if $R > 0.6$, for $\alpha = 2$ if $R > 0.7$, and for $\alpha = 1$ if $R > 0.8$.

FCG rates *da/dN* predicted by the proposed algorithm are compared with 7075-Al alloy data measured in a wide ΔK range at two stress ratios, $R = 0.1$ and $R = 0.7$ (Durán et al., 2003), as shown in Fig. 5. Ferreira et al. (2017) describe this comparison in detail, but it can be stated here that the curves are indeed numerical predictions, not a result of any data-fitting procedure. Hence, Fig. 5 certainly indicates that the SYM used here can describe the FCG behavior of this material under CAL. The better agreement between the predictions and the FCG data obtained by using $\alpha = 3$ in the calculations is related to the plane strain FCG conditions in which Durán's data was measured.

VAL conditions are simulated as shown in Figs. 6-9, to verify how the model can predict memory effects induced by single overloads and by combinations of overloads-underloads, considering the subsequent behavior of the crack-opening stress. The model parameters and the applied loads are similar to those used by de Koning and Liefting (1988), in order to compare both results: the flow stress is 415MPa, the Young's modulus 70GPa, Poisson's ratio 0.3, and the constraint factor 1, assuming plane stress conditions.

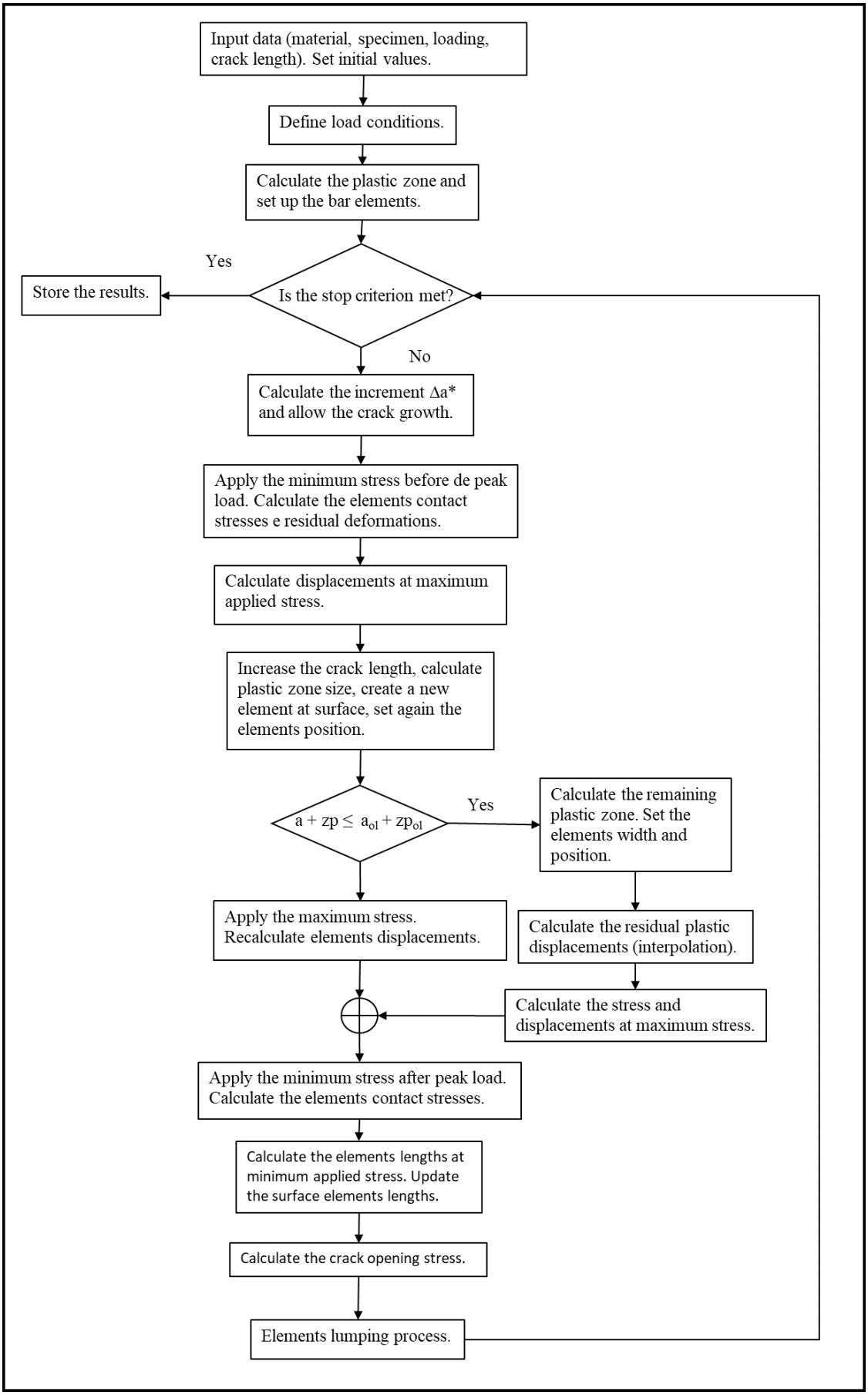

Figure 3: Flow diagram for the strip yield model.

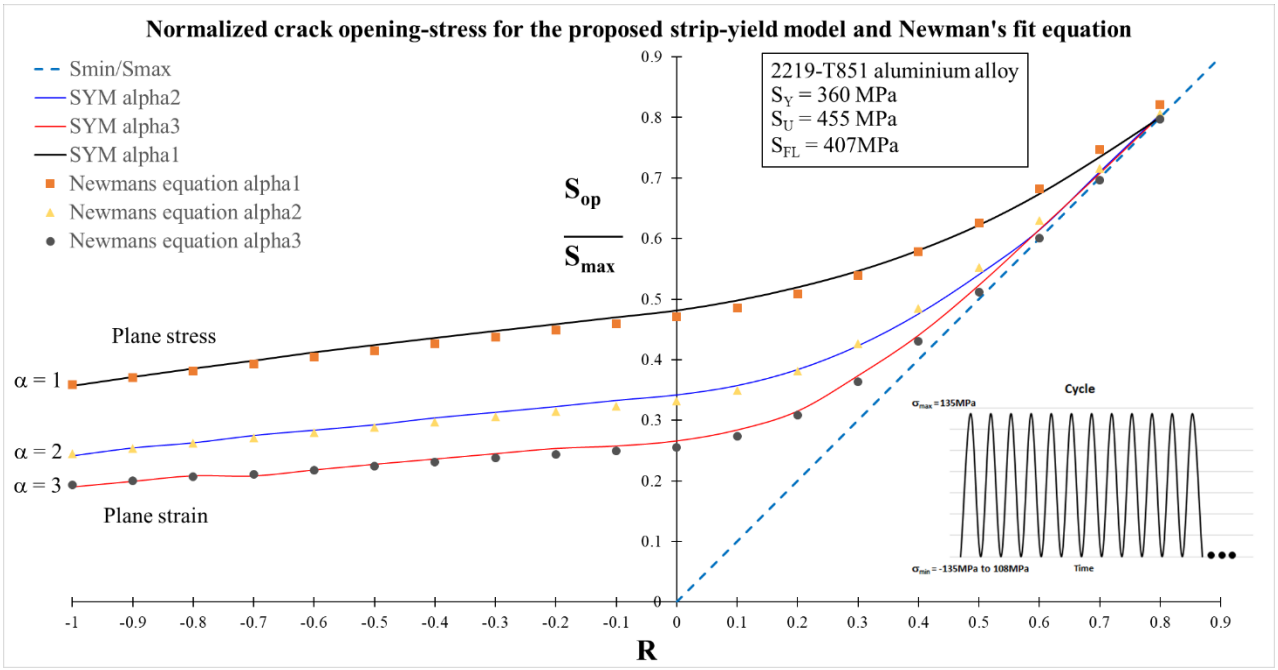

Figure 4: Proposed SYM against Newman's fit equation.

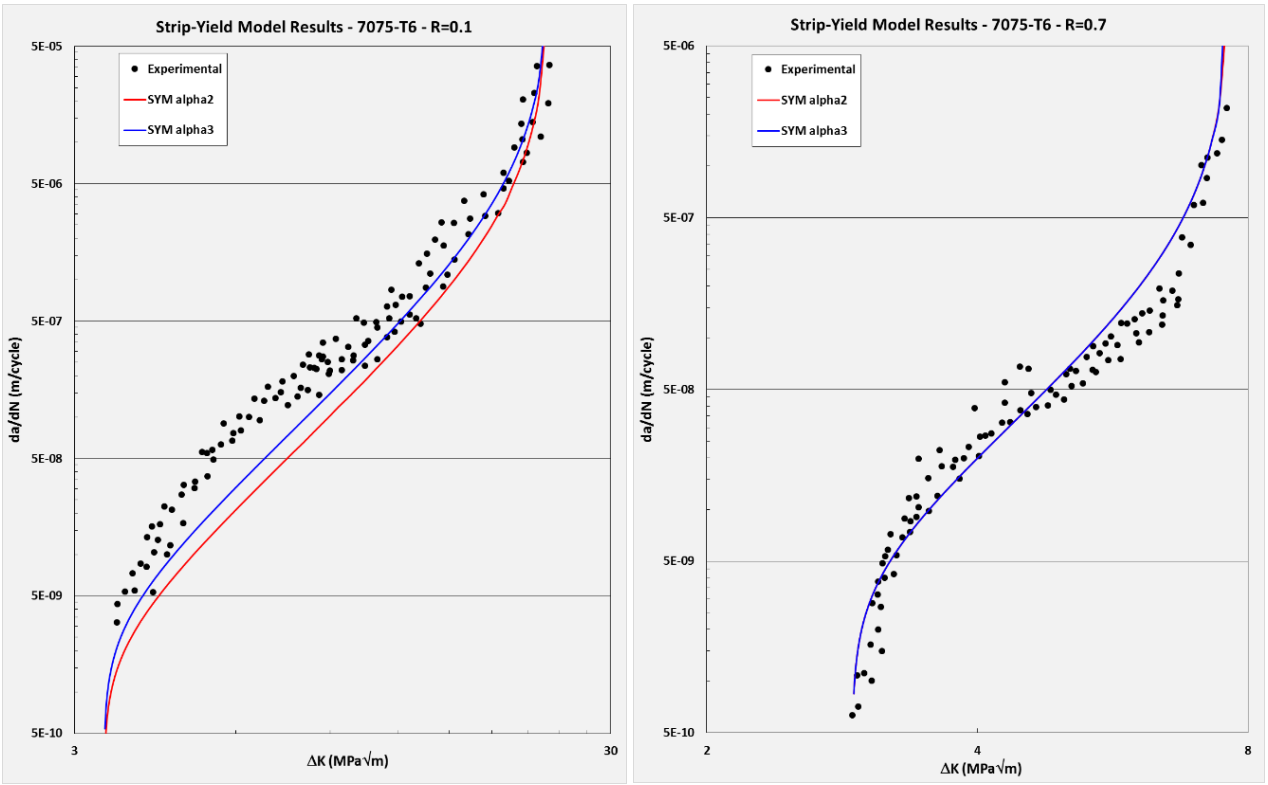

Figure 5: Algorithm results for (a) R=0.1 and (b) R=0.7.

The effect of the residual plastic deformations left on the crack surface before the overload is analyzed in Fig. 6. For three different crack surface conditions, the crack-opening stress resulting from the application of a single overload of 160MPa is the same. The general crack-opening stress behavior from the proposed SYM is similar to the behavior described by de Koning and Liefting (1988), with a small difference on the size of the zone affected by the overload. Results from de Koning and Liefting (1988) predict this zone should be about 0.3mm, whereas the proposed algorithm predicts it should be about 0.5mm.

In fact, the monotonic plastic zone for the overload (160MPa) is 1.08mm and for the subsequent load cycle (120MPa) is 0.57mm, a difference of about 0.5mm. Hence, the affected zone size predicted by the proposed model properly reproduces Führing and Seeger's (1979) memory rule.

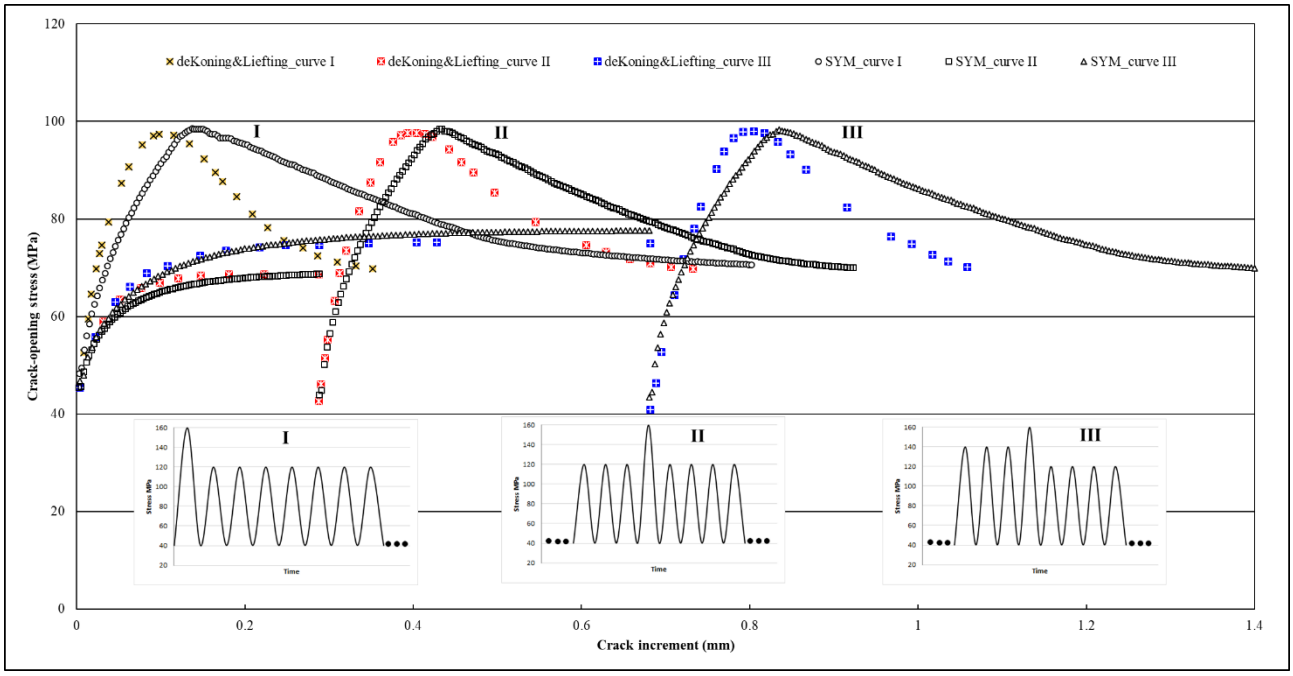

Figure 6: The effect of different plastic wakes on the crack-opening stress after a single overload.

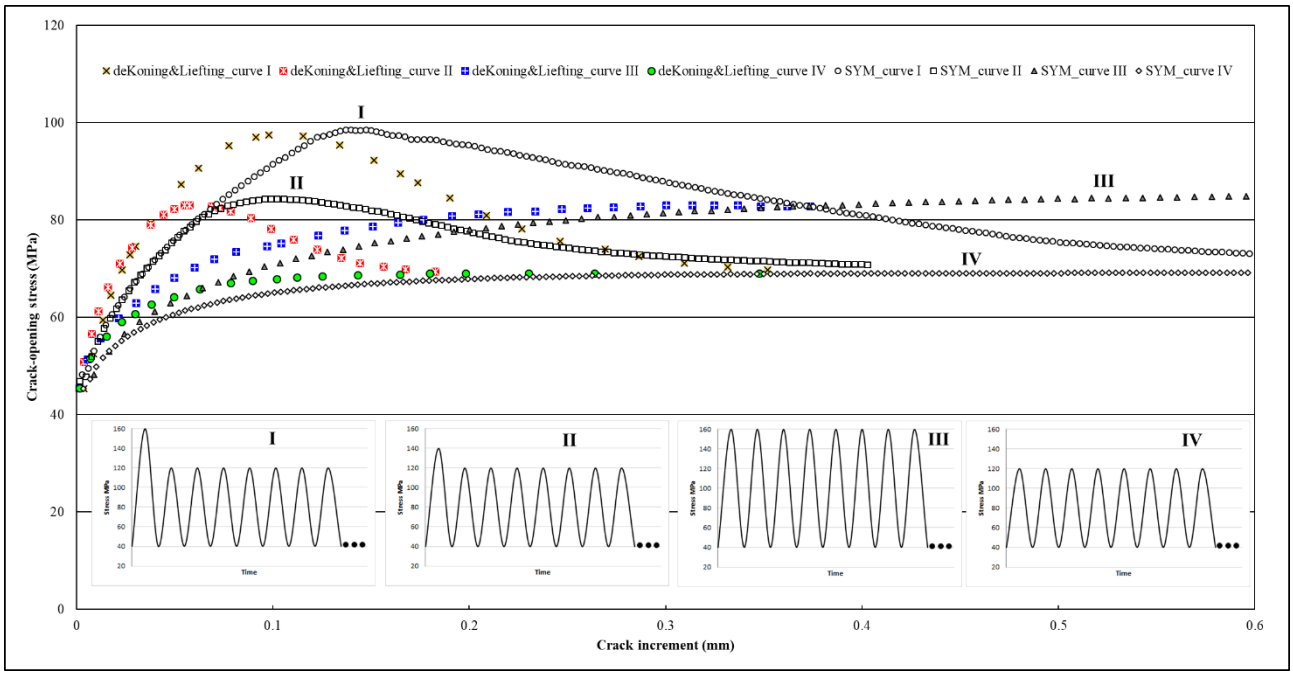

Figure 7: The effect of the overload level on the crack-opening stress.

A similar behavior is observed in Fig. 7, where the effect of the overload (OL) amplitude is analyzed. As it could be expected, an increase in the overload level, while keeping the amplitude of the subsequent CAL cycles, increases the crack-opening peak stress and the affected zone size too, inducing a higher retardation effect on the OL-affected FCG.

The effect of an underload event applied after the overload is analyzed in Fig. 8. The size of the region affected by the overload is not changed by the application of the underload, as shown by curves II and IV. The crack opening stress decreases with the underload level, and for the overload-underload ratio R = –1 (curve III) the beneficial effect of the overload is completely removed. The expected behavior of the crack-opening load after the underload application is predicted by the proposed SYM algorithm and reproduces the results reported by de Koning and Liefting (1988).

The main difference between the results reported here and those reported by de Koning and Liefting is again in the size of the overload-affected region – always superior according to the memory criterion adopted in the proposed algorithm. The peak crack-opening stress was lower by 6% in curve II and by 4% in curve IV, as compared with the results reported by de Koning and Liefing (1988).

The effect of changes in the upper load level of the CAL applied following a single overload is illustrated in Fig. 9. As expected, the size of the affected zone and the crack-opening peak stress decrease with the upper level of the CAL cycles after the overload, as shown by curves I, II and III. Once again, the FCG behavior predicted by the proposed model is similar to the behavior predicted by de Koning and Liefting (1988).

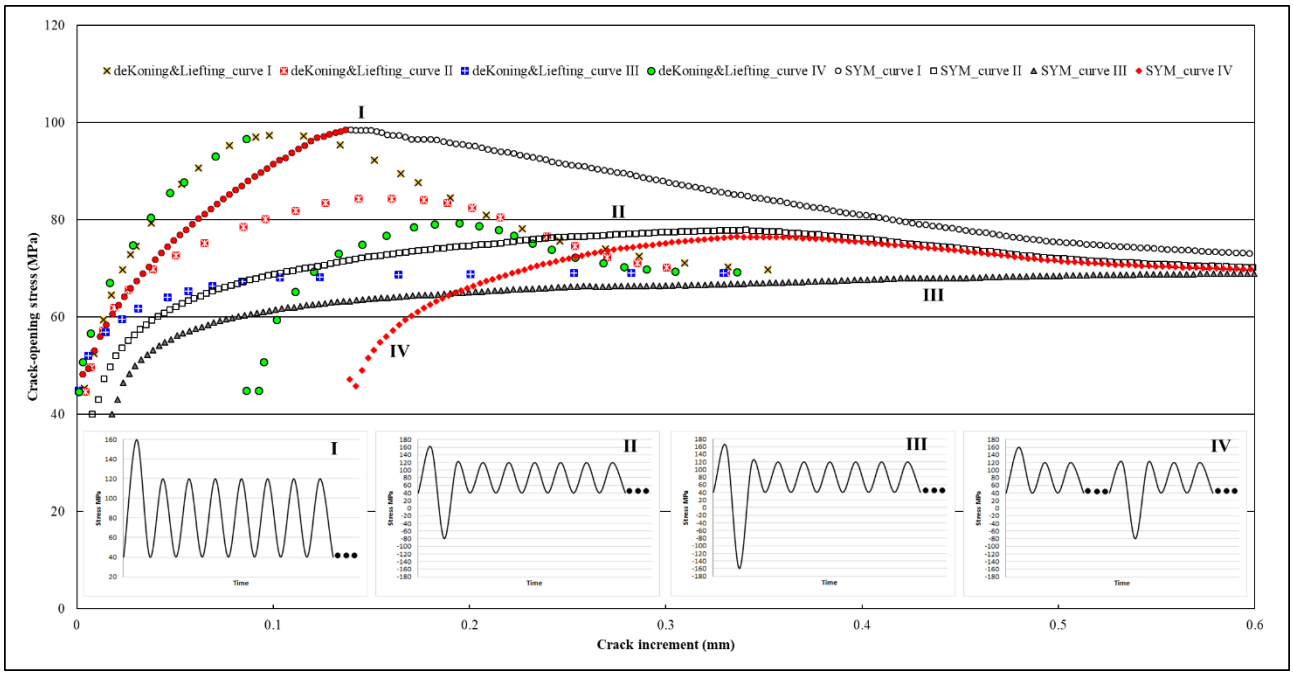

Figure 8: The effect of the underload level on the crack-opening stress.

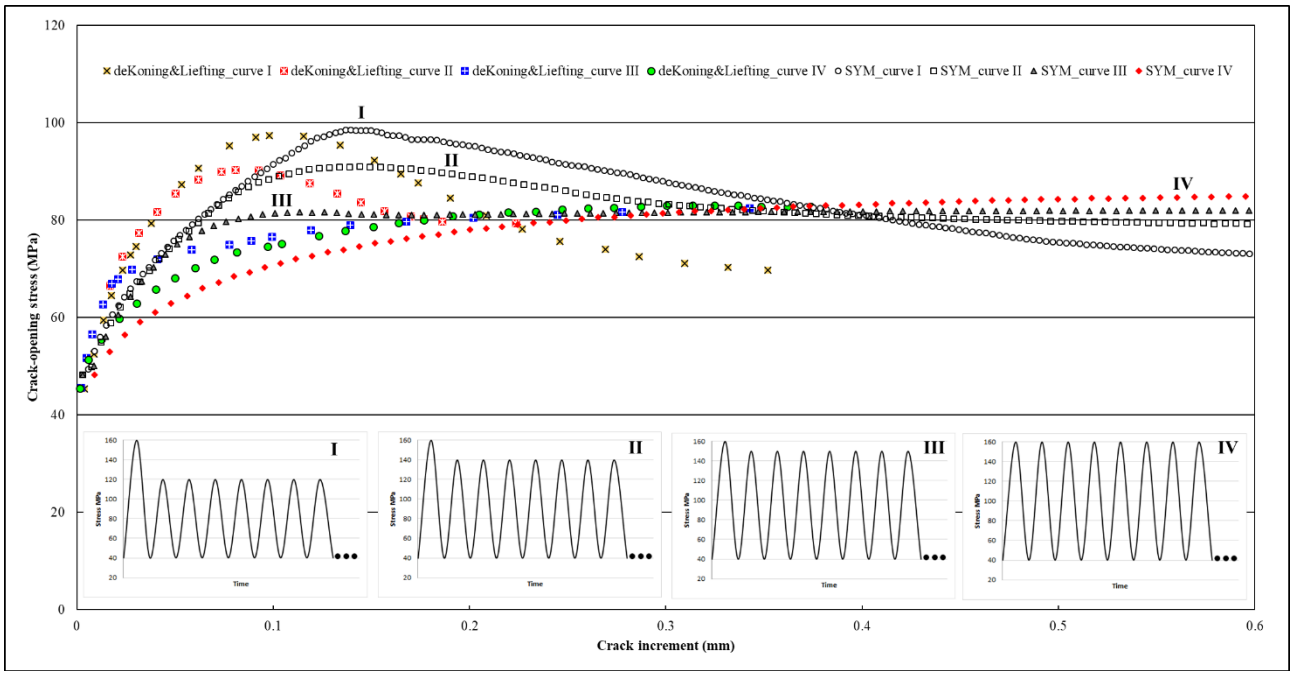

Figure 9: The effect of the upper CAL level on the crack-opening stress.

4. CONCLUSION

A SYM algorithm to calculate the crack-opening stress and estimate FCG rates under CAL and VAL is proposed and described in detail. It uses equations developed by Newman (1981, 1992) with a proper calculation procedure. Memory effects induced by VAL are estimated by the rules proposed by Füring and Seeger (1979), and with them the proposed algorithm simulates single OL and OL followed by UL effects in the same way similar algorithms reported in the literature

do. Finally, the proposed algorithm is validated using Newman's fit equation (1992) for CAL and the results reported by de Koning and Liefting (1988) for VAL.

5. REFERENCES

de Koning, A.U., Liefting, G., 1988. Analysis of Crack Opening Behavior by Application of a Discretized Strip Yield Model, Mechanics of Fatigue Crack Closure, ASTM STP 982, pp. 437-458.

Dill, H.D., Saff, C.R., 1976. Spectrum crack growth prediction method based on crack surface displacement and contact analyses, ASTM STP 595: 306-319.

Dugdale, D.S., 1960. Yielding of sheets containing slits. J Mech Phys Solids 8:100-104.

Durán, J.A.R., Castro, J.T.P., Filho, J.C.P., 2003. Fatigue crack propagation prediction by cyclic plasticity accumulation models, Fatigue and Fracture Eng. Mat. Structures, 26, 137-150.

Elber, W., 1971. The significance of fatigue crack closure. Damage Tolerance in Aircraft Structures, ASTM STP 486:230-242.

Führing, H., Seeger, T., 1979. Structural memory of cracked components under irregular loading. Fracture Mechanics, ASTM STP 677:144-167.

NASGRO, 2002. Fracture Mechanics and Fatigue Crack Growth Analysis Software, Reference Manual, version 4.02.

Meggiolaro, M.A., Castro, J.T.P., 2003. On the dominant role of crack closure on fatigue crack growth modeling. Int J Fatigue 25:843-854.

Newman Jr, J.C., 1992. FASTRAN II: a fatigue crack growth structural analysis program, NASA Technical Memorandum 104159, LRC Hampton.

Newman Jr, J.C., 1981. A crack-closure model for predicting fatigue crack growth under aircraft spectrum loading, ASTM STP 748:53-84.

Skorupa, M., 1998. Load interaction effects during fatigue crack growth under variable amplitude loading - a literature review - part I: empirical trends. Fatigue Fract Eng Mater Struct 21:987-1006.

Skorupa,M., 1999. Load interaction effects during fatigue crack Growth under variable amplitude loading - a literature review - part II: qualitative interpretation. Fatigue Fract Eng Mater Struct 22:905-926.

Vasudevan, A.K., Sadananda, K., Holtz, R.L., 2003. Unified approach to fatigue damage evaluation. NRL Review:51-57.

Wang, G.S., Blom, A.F., 1991. A strip model for fatigue crack growth predictions under general load conditions. Eng. Fract. Mechanics 40:507-533.

6. RESPONSIBILITY NOTICE

The authors Samuel Elias Ferreira, Jaime Tupiassú Pinho de Castro and Marco Antonio Meggiolaro are the only responsible for the printed material included in this paper.